

# Investigations on Dielectric Resonator Material $(\text{Ba}/\text{Ca})_2\text{Ti}_9\text{O}_{20}$ for Microwave Communication Technology

ANAND K TYAGI

Centre for Materials Research,  
SBS State Technical Campus,  
NH-95, Firozpur 152004,  
INDIA  
[akt@aol.in](mailto:akt@aol.in), [www.sbsstc.ac.in](http://www.sbsstc.ac.in)

**Abstract:** Dielectric Resonators have recently attained a great importance in microwave/ mobile communication technology due to their promising characteristics, higher degree of versatility and better frequency stability. Complex Barium Titanate ( $\text{Ba}_2\text{Ti}_9\text{O}_{20}$ ) is an important Dielectric Resonator material for microwave communication technology. The present study reports on synthesis of these materials by using the powders derived from Internal Combustion Method. Ca doped single phase materials with nominal composition  $(\text{Ba}_{1-x}\text{Ca}_x)_2\text{Ti}_9\text{O}_{20}$  ( $0.0 \leq x \leq 0.1$ ) have been successfully fabricated in present study. The phase development is found to be a two-step process; first the production of nanocrystalline powders of intermediate phases and second the metallurgical reaction among these nano-powders after consolidation followed by pyroprocessing. This method is found to produce the desired ceramic phase at a lower calcinations temperature in a surprisingly shorter time as compared to the earlier studies reported in literature. The synthesized phase pure materials are found to have improved characteristics that make them suitable to be used as Dielectric Resonator in Microwave/Mobile Communication Technology. Moreover, the dielectric characteristics of these materials are found to be highly sensitive to process parameters like particle size and pH value.

**Keywords:** - Barium Titanate, Dielectric Resonator, Internal Combustion, nano-materials

## 1 Introduction

The Microwave/Mobile Communication has witnessed a many-fold growth during the last decade technological advancement owes to the availability of suitable electroceramics that function as the important circuit elements, like filters, oscillators with selectable frequencies, amplifiers and tuners that are less expensive and technologically efficient. In the present work, we have synthesized the ceramic based Dielectric Resonators (DRs) that are used as modern substitutes to the Resonant Cavities in microwave communication systems. DRs have attracted attention of the scientific community since last few years as a result there had been an unprecedented development and growth in this area [1-4]. Their characteristics can be easily tailored to meet specific requirements through exploiting the complex interplay between processing and chemistry, structure at many levels and device physics.

As early as in 1939, Richtmyer, R.D. [5] showed that unmetallized dielectric objects can function similar to metallic cavities which he called dielectric resonators (DRs). Practical applications of DRs to microwave circuits, however, began to appear only in the late 60's as resonating elements in waveguide filters [Cohn (1968)]. DR's have completely replaced the bulky metallic cavities in most microwave applications for reasons of cost, dimension, mass,

stability, efficiency, ruggedness and ease of use. Recent developments in ceramic material technology have resulted in a number of improvements including small controllable temperature coefficients of resonant frequency over the useful operation temperature range and very low dielectric losses at microwave frequencies. These developments have revived interest in DR applications for a wide variety of microwave circuit configurations and subsystems [7-10]. Some of the advantages of the substitution of conventional resonators by DRs are:

- Smaller circuit sizes and greater degree of circuit and subsystem integration,
- Better circuit performance, with regard to both temperature and losses.
- Reduction of overall circuit cost for comparable performances.
- Promising features i.e. High Quality (Low Dielectric Loss, High Q Value), Wide Range (Wide varieties of Dielectric Constant, Wide Frequency ranges) and Better Reliability (Excellent environmental stability, High/Good stability/linearity of temperature coefficient).

A DR is essentially an electronic component that exhibits resonance for a narrow range of frequencies, generally in

the microwave band. The resonance is similar to that of a circular hollow metallic waveguide, except that the boundary is defined by large change in permittivity rather than by a conductor. DR's are generally consisted of a "puck" of ceramic, the resonance frequency of which is determined by its overall physical dimensions and the dielectric constant of the material. The temperature coefficient of the resonant frequency can be engineered to have a desired value, to meet circuit designer's requirements.

### 1.1 Basic Material Properties

The most important material properties for DRs are their dielectric constant ( $\epsilon_r$ ), quality factor (Q), and temperature coefficient of resonant frequency ( $\tau_f$ ). The dielectric constant of the material ultimately determines the resonator dimensions. At present, commercially available temperature stable DR materials exhibit dielectric constants of about 36 to 40. The usual reason for choosing a DR as a resonating element is the size reduction afforded by the high  $\epsilon_r$  of modern ceramics. But dielectric constant is a misnomer, not only does  $\epsilon_r$  vary slightly for different temperature coefficient blends within the same material family, but lot-to-lot ceramic process variations cause  $\epsilon_r$  to swing typically  $\pm 1$  unit between lots but within a given lot, the variation is much smaller.

The unloaded Q factor ( $Q_0$ ) that depends strongly on both dielectric losses and environmental losses is defined by the ratio between the stored energy to the dissipated energy per cycle. The measure of the DR's ability to store microwave energy with minimal signal loss is its Q value. Every DR application is unique, and since the RF fields of the most commonly used modes do not end at the boundaries of the ceramic, metal wall losses will lower the Q value of the shielded DR. It's worth emphasizing that measured Q is both mode and temperature dependent. Moreover, here it is important to note that Q factor of a material can be degraded by inadvertent marking on the DR sample with graphite pencil. The temperature coefficient of resonant frequency ( $\tau_f$ ) combines three independent factors, namely temperature coefficient of the dielectric constant, thermal expansion of the material ( $\alpha_L$ ) and thermal expansion of the environment in which the resonator is mounted. There may also be shifts in resonant frequency due to intrinsic material parameters that are related to the aforesaid temperature coefficients. The time and care required to thermally stabilize the sample, as well as the mounting, makes temperature coefficient a time consuming parameter to measure. An "isolated" measurement is necessary to discern the ceramic properties from other influences.

### 1.2 Resonator Design and Tuning Modes

Among the theoretically explored geometrics, the cylindrical shape has been widely accepted as the most advantageous one [11]. The natural modes of a cylindrical sample of high

dielectric constant material can be classified into four categories:  $TE_{opg}$ ,  $TM_{opg}$ ,  $HE_{npg}$ , and  $EH_{npg}$ , where n and p are integers which describe the standing wave pattern in the azimuthal and radial directions respectively, while g is in general a real number; reflecting the fact that the two circular boundary surfaces do not contain an integer number of half wavelengths as in metallic cavities.

For the fundamental TE mode, g is usually substituted by  $\delta$  and the mode is referred as  $TE_{01\delta}$  here  $\delta$  assumes values in the range 0.5 to 1.0. TE and TM modes do not contain electric and magnetic fields in the axial directions (z) respectively. The HE and EH modes are called hybrid, because all six field components are present in both. The great majority of practical applications employ either the  $TE_{01\delta}$  mode or the  $HE_{11g}$  mode, which are the first two to resonate when the DR is placed between conducting walls and air gaps left in between. Fig.1 shows a sketch of the fields for these two modes in the cross section of the resonator. The ratio between the DR diameter and its length (D/H) together with the exterior boundary conditions such as tuning elements, holders, shields, and substrates determines which of the two modes has the lowest resonant frequency. For most configurations [12,13] the  $TE_{01\delta}$  mode is dominant when  $D/H > 1.42$ .

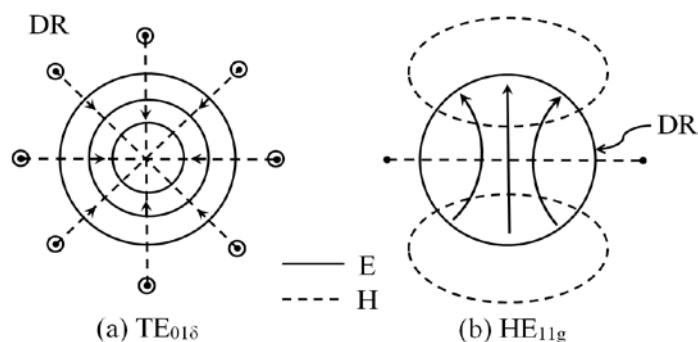


**Fig.1: Sketches of the fields for  $TE_{01\delta}$  &  $HE_{11g}$  modes in the cross-section of the resonator**

### 1.3 Resonator Materials

A good DR material must have low loss (i.e large Q value), high temperature stability with a reasonably high relative permittivity and a very small change in resonant frequency as a function of temperature. Ceramic dielectrics and ferroelectrics (i.e. dielectrics with spontaneous polarization) are the obvious choices keeping in view their characteristics and the following facts;

- Ceramics don't have age perceptibly. Any change in the resonant frequency of a DR over time can be attributed to change in the measurement cavity or measurement technique.

- Ceramics don't absorb moisture noticeably, but moisture condensation on the surface of the DR can affect Q value. The Q will recover when the moisture is driven off, for example, by self-heating of the DR.
- Ceramics chip easily with hard surfaces. Most tiny chips will not affect the electrical performance at all. Surface roughness is also not particularly important: there are no currents in a ceramic dielectric resonator, the energy is stored in the form of fields.
- Ceramics are "born" in kilns at temperatures over 1,000 °C. They can stand much higher temperatures than the electronic equipment they are used with, i.e., far in excess of soldering temperatures.

These dielectric microwave materials like simple titanate ceramics i.e. BaTiO<sub>3</sub> and its derivatives, have been investigated extensively and beside a number of research reports, a few patented technologies are also available in literature [14,15]. However the complex titanates have not been given much importance though they have enormous research and application potential. Ba<sub>2</sub>Ti<sub>9</sub>O<sub>20</sub> is one such low loss (quality factor Q>10,000), temperature stable dielectric material with a reasonably high relative permittivity (~39). It shows a very small change in resonant frequency as a function of temperature (~4 ppm/K). Therefore, it is well suited as a dielectric resonator for use in the microwave communication technology [16-18].

## 2 Synthesis of Dielectric Resonator Ba<sub>2</sub>Ti<sub>9</sub>O<sub>20</sub> Ceramics

So far, the synthesis of ceramic nanocrystalline materials has been carried out most frequently by assembling pre-generated small clusters by means of *in situ* consolidation and sintering or through some state of art processes that do not require pre-generated clusters. Thus, we shall first review the various techniques belonging to the category of condensed phase synthesis. Decomposition and precipitation reactions in ionic materials have been utilized to generate nanometer-sized clusters for most of the ceramics. For example, decomposition of Mg(OH)<sub>2</sub> and MgCO<sub>3</sub> yielded MgO clusters with about 2 nm diameter [19]. Hydrothermal reactions (reactions of the water above its boiling point) have been proposed to be applied to synthesize small clusters. The two reactions applied so far are hydrothermal precipitation and hydrothermal oxidation [20]. Both reactions yield suspensions of crystalline metal oxides in water. Simple oxides (ZrO<sub>2</sub>, SiO<sub>2</sub>, Al<sub>2</sub>O<sub>3</sub>, TiO<sub>2</sub>, MgO, CaO), as well as, mixed oxides (ZrO<sub>2</sub>-Y<sub>2</sub>O<sub>3</sub>, ZrO<sub>2</sub>-Y<sub>2</sub>O<sub>3</sub>-MgO, ZrO<sub>2</sub>-MgO, ZrO<sub>2</sub>, ZrO<sub>2</sub>-Al<sub>2</sub>O<sub>3</sub>, BaFe<sub>12</sub>O<sub>19</sub>, BaTiO<sub>3</sub>), have been prepared in the size ranges between 10 nm and 100 nm. The solution sol-gel method has also been utilized in a variety of systems to generate small (< 10 nm) clusters of SiO<sub>2</sub>, Al<sub>2</sub>O<sub>3</sub> and TiO<sub>2</sub>. Both structural and compositional nanometer

structures are obtained by "seeding" of a ceramic precursor with crystalline sols of the final equilibrium phase to catalyze nucleation [21,22].

### 2.1. Review of earlier works

The fabrication of very dense bodies of Ba<sub>2</sub>Ti<sub>9</sub>O<sub>20</sub> ceramic with phase purity is of great practical importance for improvement in dielectric characteristics. The realization of monophasic Ba<sub>2</sub>Ti<sub>9</sub>O<sub>20</sub> had, however, been a challenge and there are only a few reports available on the topic [23,24]. A solid state reaction between BaCO<sub>3</sub> and TiO<sub>2</sub> even at 1360°C for 5 hours could not get the monophasic Ba<sub>2</sub>Ti<sub>9</sub>O<sub>20</sub> [25]. However, synthesis of a near monophasic Ba<sub>2</sub>Ti<sub>9</sub>O<sub>20</sub> has been obtained by a rapid thermal processing of BaTiO<sub>3</sub> and TiO<sub>2</sub> at 1390°C [26]. The formation of unwanted phases is more common during the fabrication of the complex mixed oxide phases such as barium polytitanates that can be avoided by an intimate blending of the constituents during the synthesis of these materials.

The investigations into the mechanism of formation of barium titanate Ba<sub>2</sub>Ti<sub>9</sub>O<sub>20</sub> phase in the BaO-TiO<sub>2</sub> and BaO-SrO-TiO<sub>2</sub> systems [27,28] using initial mixtures prepared by three methods, namely, mechanical grinding of the initial reactants, coprecipitation from aqueous solutions of salts, and the sol-gel technique revealed that, irrespective of the preparation procedure, the formation of Ba<sub>2</sub>Ti<sub>9</sub>O<sub>20</sub> proceeds through the formation of the intermediate phases BaTi<sub>4</sub>O<sub>9</sub> and BaTi<sub>5</sub>O<sub>11</sub> [27]. The nature of the intermediate phases is determined by the homogeneity and dispersion of the initial mixture, as well as by the stability of the intermediate phase. The most optimum conditions for the synthesis of Ba<sub>2</sub>Ti<sub>9</sub>O<sub>20</sub> [28] are provided by the formation of BaTi<sub>5</sub>O<sub>11</sub> as an intermediate phase upon heat treatment of the coprecipitation products in the nanocrystalline state. The metastability and structural defects in the BaTi<sub>5</sub>O<sub>11</sub> intermediate phase encourage a decrease in the temperature of the final heat treatment by 100-150°C in the course of the preparation of Ba<sub>2</sub>Ti<sub>9</sub>O<sub>20</sub> single-phase ceramics. The study on formation of Ba<sub>2</sub>Ti<sub>9</sub>O<sub>20</sub>-based phases in the course of solid-phase interaction in the BaO-TiO<sub>2</sub>(ZrO<sub>2</sub>) and Cs<sub>2</sub>O-BaO-TiO<sub>2</sub>(ZrO<sub>2</sub>) Systems also showed the similar findings that the formation of the Ba<sub>2</sub>Ti<sub>9</sub>O<sub>20</sub> compound and Ba<sub>2</sub>Ti<sub>9</sub>O<sub>20</sub>-based solid solutions, is a multistage process [29] proceeding through the formation of intermediate phases. The solid-phase interaction in the BaO-TiO<sub>2</sub>(ZrO<sub>2</sub>) system occurs through the formation of the BaTi<sub>4</sub>O<sub>9</sub> intermediate compound [30]. The Ba<sub>2</sub>Ti<sub>9</sub>O<sub>20</sub> single-phase product is formed only in the presence of ZrO<sub>2</sub> (0.82 mol %) upon heat treatment at a temperature of 1250°C for 5 h. In the Cs<sub>2</sub>O-BaO-TiO<sub>2</sub>(ZrO<sub>2</sub>) system, the BaTi<sub>5</sub>O<sub>11</sub> metastable

intermediate phase is formed at the first stage of the solid-phase interaction. The  $Cs_xBa_{2-x/2}Ti_{9-y}Zr_yO_{20}$  single-phase solid solutions are prepared upon heat treatment at 1100°C for 1 h. It is demonstrated that, in the  $Ba_2Ti_9O_{20}$  structure, cesium can isomorphously substitute for barium with the formation of  $Cs_xBa_{2-x/2}Ti_{9-y}Zr_yO_{20}$  solid solutions ( $0 \leq x \leq 0.8$ ,  $y = 0$  and 0.09). The identical study on formation of  $Ba_2Ti_9O_{20}$  ceramics from EDTA-gel-derived powders [31] established that intermediate phases play a vital role at the preparation stage of these materials. The development of glassy and semicrystalline phases in the  $BaO-B_2O_3-TiO_2$  system [32] and Sintering  $BaTi_4O_9/Ba_2Ti_9O_{20}$ -based ceramics by glass addition [33] have also been reported in literature.

The thermal processing of  $BaTi_4O_9$  and  $Ba_2Ti_9O_{20}$  dielectric resonators by sintering the pressed powder pellets of Sn-doped and undoped barium titanates at 1360 and 1390°C for 5 h respectively, though batched to form  $Ba_2Ti_9O_{20}$ , revealed a two-phase microstructure of  $BaTi_4O_9$  and  $TiO_2$  formed in the undoped system [34]. The dielectric constant at 6 GHz was 40 without  $SnO_2$  additions. Doping with 1.64 mol %  $SnO_2$  stabilized  $Ba_2Ti_9O_{20}$  and formed a single-phase microstructure but resulted in higher porosity. Dilatometry studies implied that  $SnO_2$  additions facilitated a greater fraction of reaction to occur in the solid state, causing a lower quantity of pore-filling fluid to form above 1317°C. As a result of the higher porosity, the dielectric constants and quality factors were found to reduce. However, the rapid thermal processing of  $BaTi_4O_9$  and  $TiO_2$  pressed powders at 500 °C/min to 1250 °C for 2 h in an infrared furnace resulted in a mixture of  $BaTi_4O_9$ ,  $Ba_2Ti_9O_{20}$  and  $TiO_2$  [26]. Further heat treatment at 1390°C led to 96 vol% phase-pure  $Ba_2Ti_9O_{20}$  from an initial mixture devoid of any dopant. Heat treatment at rates decreasing to 5 °C/min facilitated agglomeration of  $TiO_2$ . This, in turn, increased the diffusion distance required for reaction of  $BaTi_4O_9$  and  $TiO_2$  to form  $Ba_2Ti_9O_{20}$ .

The studies on phase evolution, grain size and dielectric properties of Sol-Gel derived  $BaTi_4O_9$  and  $B_2O_3$ -doped  $Ba_2Ti_9O_{20}$  ceramics powders [35] showed that the  $BaTi_4O_9$  and 5 wt%  $B_2O_3$ -doped  $Ba_2Ti_9O_{20}$  ceramics powders calcined at 800°C for 2 h have the grain sizes of 30–80 and 50–200 nm, respectively. Monophase sample of  $BaTi_4O_9$  with orthorhombic symmetry could be obtained after the  $BaTi_4O_9$  precursor was calcined at 1200°C for 2 h, whereas, monophase sample of 5 wt%  $B_2O_3$ -doped  $Ba_2Ti_9O_{20}$  was obtained at 800°C for 2 h. The  $BaTi_4O_9$  and  $Ba_2Ti_9O_{20}$ : 5 wt%  $B_2O_3$  ceramics fabricated using the sol-gel powders were found to have microwave dielectric properties with  $\epsilon_r = 36.1$ ,  $Q = 3220$  at 5.31 GHz, and  $\epsilon_r = 34.5$ ,  $Q = 2425$  at 5.53 GHz, respectively. The fine powders of these ceramics have also been fabricated by emulsion process [36] but the particle size obtained are much larger.

The synthesis of  $Ba_2Ti_9O_{20}$  phase via acid precursor has been reported using the modified Pechini method [37] with ethylene diamine tetra acetic acid as a chelating. The resin precursors were prepared and heated at 700 to 1200 °C in air, and x-ray diffraction was used to determine the phase transformations as a function of temperature. Single-phase  $Ba_2Ti_9O_{20}$  was obtained at 1200 °C for 2-6 h, without the need of prolonged heat treatment time. The process was simple and easy to control: low-temperature conditions or a protective atmosphere was not needed. Differential thermal analysis, thermogravimetric analysis, and Raman spectroscopy were used to characterize the precursors and derived oxide powders. The single Phase  $Ba_2Ti_9O_{20}$  Microwave Dielectric Ceramics have also been prepared by low temperature liquid phase sintering by adding  $PbO-B_2O_3-SiO_2$  (PBS) as a liquid phase sintering aid [38]. With the addition of 5 wt% PBS, dense and single-phase  $Ba_2Ti_9O_{20}$  dielectric resonators could be fabricated at a sintering temperature below 1200°C. The microwave dielectric properties of PBS-  $Ba_2Ti_9O_{20}$  ceramics were found to depend upon the density, the amount of liquid phase and the sintering temperature. Although glass addition results in a decrease of the dielectric properties, the sintered PBS-  $Ba_2Ti_9O_{20}$  ceramics still exhibit much better dielectric properties than that of pure  $Ba_2Ti_9O_{20}$  ceramics at low sintering temperatures [38].

Single phase  $Ba_2Ti_9O_{20}$  has also been prepared by using the powder derived from an auto-ignition route [39]. This method involves an exothermic decomposition of a fuel oxidant precursor and results in either the finely divided powder with required phase or semi-decomposed precursor with a considerable carbonaceous residue [40-44].

## 2.2 Essentials for Synthesis of $Ba_2Ti_9O_{20}$

The fabrication of very dense bodies of  $Ba_2Ti_9O_{20}$  ceramic with phase purity is of great practical importance for improvement in dielectric characteristics of this class of electroceramics. As evident from above, realization of monophasic  $Ba_2Ti_9O_{20}$  had been a challenge. The synthesis of phase pure  $Ba_2Ti_9O_{20}$  materials with improved characteristics (i.e. narrow particle size distribution among the nano-crystallites, higher surface area and better sinterability) the processes employed at synthesis step are of vital significance. For these electroceramics, the dielectric characteristics are highly sensitive to the particle size, impurity phases and porosity in the sintered products. Technical advancements in the processing of materials, especially in the micro/nano regime, have led to novel ways of creating submicron phases. Recent research has pointed out that these materials at the micro to nano scale exhibit

a length scale dependence of properties. At the nanometer scale, conditions required for nucleation and growth of one phase from another can be substantially different from those conditions at bulk scales. Here it is important to note that conventional solid state reaction between  $\text{BaCO}_3$  and  $\text{TiO}_2$  even at  $1360^\circ\text{C}$  for 5 hours is not sufficient to produce a monophasic  $\text{Ba}_2\text{Ti}_9\text{O}_{20}$ .

Though a number of systemic studies have been reported on synthesis of these materials but there remains some unanswered criticalities like optimized fabrication methodology, control over particle size, interfacial effects, micro-structural stability aspects versus improvement in characteristics, environmental and aging impacts on the materials. Synthesis of near monophasic  $\text{Ba}_2\text{Ti}_9\text{O}_{20}$  can be achieved only through a Novel Synthesis route. It has been reported in literature that formation of barium nona titanate  $\text{Ba}_2\text{Ti}_9\text{O}_{20}$  phase may be realized using the following methods;

- Mechanical grinding of the initial reactants,
- Coprecipitation from aqueous solutions of salts,
- Sol-gel technique,
- Acid precursor, the modified Pechini method,
- Low temperature liquid phase sintering and
- Internal Combustion/Auto-Ignition method

During recent years Internal Combustion Method (ICM) has emerged as a popular tool for synthesizing the advanced ceramics, composites, intermetallics and alloys, nanomaterials and some state of art catalysts also [1-3]. This method involves an exothermic decomposition of a fuel oxidant precursor and results in either the finely divided powder with required phase or semi-decomposed precursor with a considerable carbonaceous residue. The powder characteristics obtained by this technique are primarily dependent on the enthalpy or the flame temperature generated during ignition hence this method is referred as Internal Combustion (IC). Depending upon the nature of reactants: elements or compounds (solid, liquid or gas) this process of exothermicity may have a number of names like Self-propagating High Temperature Synthesis, Low Temperature Combustion Synthesis, Solution Combustion Synthesis, Gel Combustion, Sol-Gel Combustion, Emulsion Combustion, Volumetric Combustion, Thermal Explosion etc.

Combustion synthesis processes are characterized by high-temperatures, fast heating rates and short reaction times. These features make ICM an attractive method for manufacturing technologically useful materials at lower costs compared to conventional ceramic processes. Some other advantages of this method are; i) Cost effective process with simple instruments, ii) High Purity Contamination free end

products, iii) Capability to synthesize materials that are otherwise very difficult to make and iv) Effective control over process parameters.

## 3 Results and Discussion

### 3.1 Synthesis of Ca Doped Monophasic $\text{Ba}_2\text{Ti}_9\text{O}_{20}$

In present study Ca doped single phase  $\text{Ba}_2\text{Ti}_9\text{O}_{20}$  with nominal composition  $(\text{Ba}_{1-x}\text{Ca}_x)_2\text{Ti}_9\text{O}_{20}$  ( $0.0 \leq x \leq 0.1$ ), henceforth referred as  $(\text{Ba}/\text{Ca})_2\text{Ti}_9\text{O}_{20}$  has been prepared by using the powder derived from an Auto-Ignition/Internal Combustion route. This method is capable of producing the nanocrystalline powders of the oxide ceramics at a lower calcinations temperature in a surprisingly shorter time. Synthesis of phase pure  $\text{Ba}_2\text{Ti}_9\text{O}_{20}$  materials with improved characteristics is facilitated by narrow particle size distribution among the nano-crystallites produced, higher surface area, and better stability. For these electro-ceramics, the dielectric characteristics are highly sensitive to the particle size, impurity phases and porosity. Technical advancements in the processing of materials, especially in the micro/nano regime, have led to novel ways of creating submicron phases. Recent research has pointed out that these materials at the micro to nano scale exhibit a length scale dependence of properties. At the nanometer scale, conditions required for nucleation and growth of one phase from another can be substantially different from those conditions at bulk scales.

This work attempts to investigate the role of process parameters on synthesis of monophasic  $(\text{Ba}/\text{Ca})_2\text{Ti}_9\text{O}_{20}$  ceramics using the nano-phase derived powders. This technique involves an exothermic decomposition of a fuel oxidant precursor and results in either the finely divided powder with required phase or semi-decomposed precursor with a considerable carbonaceous residue. By adjusting the pH of citrate-nitrate solution, gelation is achieved through thermal dehydration. The auto-ignition of the gel at an external temperature of nearly  $240^\circ\text{C}$  is found to produce a nano-crystalline powder of  $(\text{Ba}/\text{Ca})\text{Ti}_4\text{O}_9$  and  $\text{TiO}_2$  with particle sizes in the range of 50 to 100 nm.

AR grade  $\text{TiO}(\text{NO}_3)_2$ ,  $\text{Ba}(\text{NO}_3)_2$ ,  $\text{Ca}(\text{NO}_3)_2$ , citric acid ( $\text{C}_6\text{H}_8\text{O}_7 \cdot \text{H}_2\text{O}$ ) and  $\text{NH}_4\text{OH}$  were used as the starting materials.  $\text{TiO}(\text{NO}_3)_2$  was prepared by precipitation of  $\text{TiCl}_4$  as hydrated titania using  $\text{NH}_4\text{OH}$  and dissolving the precipitate in a minimum volume of 1.4 M  $\text{HNO}_3$ .  $\text{Ba}(\text{NO}_3)_2$  and  $\text{Ca}(\text{NO}_3)_2$ , in appropriate ratio, were dissolved in hot water and cooled to room temperature. The required volume of  $\text{TiO}(\text{NO}_3)_2$  solution was mixed into the solution of  $\text{Ba}(\text{NO}_3)_2$  and  $\text{Ca}(\text{NO}_3)_2$  maintaining the  $(\text{Ba}+\text{Ca})$  to  $\text{Ti}$  molar ratio of 1:4.5. The citric acid

crystals were then added to the solution while maintaining the total metal ions to citric acid molar ratio as 1:0.5. A transparent aqueous citrate–nitrate solution is obtained. Dilute  $\text{NH}_4\text{OH}$  was then slowly added into this solution to adjust its pH value. Highly viscous yellowish gel precursors are then prepared with 3 different pH values of 2.0, 3.5 and 6. Transparency condition of the gels obtained depends on the nature of the fuel used, its amount, and pH of the starting solution. The thermal dehydration of all of them was then done on hot plate at  $\sim 90^\circ\text{C}$ . The temperature of the hot plate was then raised to  $\sim 240^\circ\text{C}$ . The gel at this temperature swelled and got ignited with an evolution of a large volume of gaseous products. The auto-ignition, which remained for  $\sim 5$  seconds, resulted in a voluminous powder. This powder was then calcined at  $600^\circ\text{C}$  for 2 hours to remove the leftover carbonaceous residue. The crystallite size in this powder was very fine ( $<50$  nm).

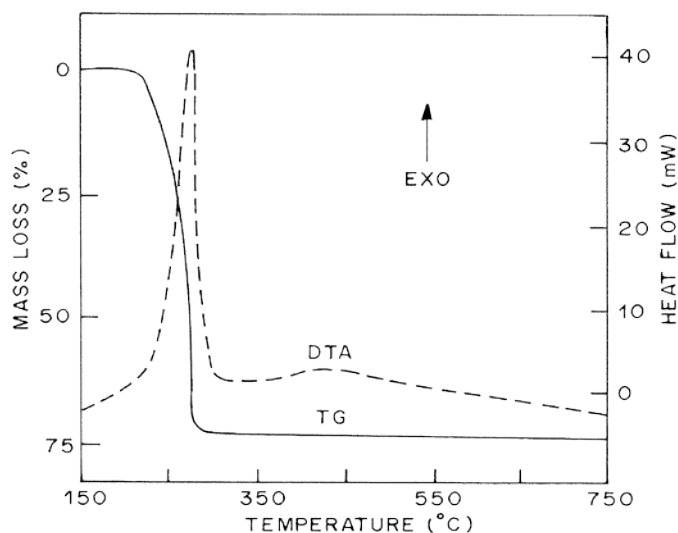


**Fig.2: Thermo-Analytical Investigations on dried yellowish gel precursor.**

### 3.2 Thermo-Analytical Study

Simultaneous TG/DTA was performed on dried yellowish gel under dynamic air atmosphere, with a heating rate of  $10^\circ/\text{min}$ . using a Leinsis Simultaneous TG/DTA/DSC instrument, Model L-81. These studies were done in order to ascertain the decomposition behavior and to know the minimum value of calcination temperature. TG/DTA curve of the dried 1:0.5 precursor gel shows a near single step exothermic decomposition at  $\sim 240^\circ\text{C}$  (Fig.2). More than 95% of the total weight loss occurs during this step of auto-ignition. The calcined powders were then cold pressed in the form of pellets with 10 mm diameter and 5-6 mm height using a hydraulic press under a compaction pressure of 4 ton/cm<sup>2</sup>. The green pellets were then sintered in dynamic air atmosphere at (a)  $1000^\circ\text{C}$  for 4 hr. (b)  $1200^\circ\text{C}$  for 2 hr. and (c)

$1250^\circ\text{C}$  for 30 min. to obtain the highly sintered mass of the material.

### 3.3 X-Ray Diffraction Study

XRD patterns of the powder obtained after auto-ignition 1:0.5 precursor gel (a) uncalcined powder (b) powder calcined at  $1000^\circ\text{C}$  and (c) sintered Sample at  $1200/1250^\circ\text{C}$  were recorded using a Bruker D-8 ADVANCE diffractometer with graphite monochromated  $\text{Mo K}_\alpha$  radiation ( $\lambda = 0.71073 \text{ \AA}$ ) XRD studies were done to investigate the phase evolution from the powder obtained after the auto-ignition as a function of calcination temperature. The uncalcined powder shows the characteristic peaks of  $(\text{Ba}/\text{Ca})\text{Ti}_4\text{O}_9$  and  $\text{TiO}_2$ . The powder obtained after calcination at  $600^\circ\text{C}$ , to remove the small amount of the residual carbonaceous material, also showed a similar kind of XRD pattern. The characteristics peaks of  $(\text{Ba}/\text{Ca})_2\text{Ti}_9\text{O}_{20}$  phase started to appear at  $900^\circ\text{C}$  and their intensity increased as a function of calcination temperature with a continuous reduction of  $(\text{Ba}/\text{Ca})\text{Ti}_4\text{O}_9$  phase. The XRD pattern of the powder calcined at  $1000^\circ\text{C}$  for 4 hrs, shows a mixture of  $(\text{Ba}/\text{Ca})\text{Ti}_4\text{O}_9$ ,  $(\text{Ba}/\text{Ca})_2\text{Ti}_9\text{O}_{20}$  and  $\text{TiO}_2$  phases. The XRD patterns of the samples sintered at  $1200^\circ\text{C}$  for 2 hrs. or at  $1250^\circ\text{C}$  for 30 min. are identical with no detectable impurities (Fig.3).

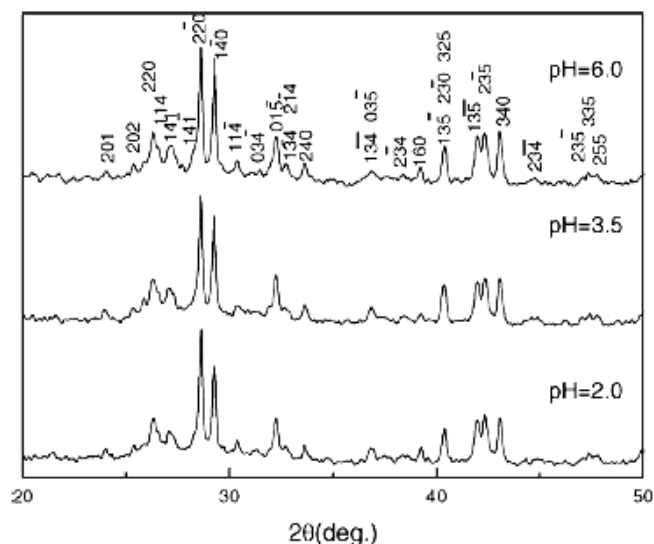


**Fig.3: XRD patterns of  $(\text{Ba}/\text{Ca})_2\text{Ti}_9\text{O}_{20}$  Gel Precursors Obtained at Different pH values and Sintered at  $1200^\circ\text{C}$  for 2 hrs.**

It is evident from Fig.3, that pH value of the nitrate-citrate solution has got a direct effect on advent of  $(\text{Ba}/\text{Ca})_2\text{Ti}_9\text{O}_{20}$  phase. Thus the optimum conditions required to have monophasic  $(\text{Ba}/\text{Ca})_2\text{Ti}_9\text{O}_{20}$  materials are pH value  $\sim 6$  and minimum temperature of either

1200°C with 2 hrs. retention or 1250°C with 30 min. retention time.

### 3.4 SEM Micrography

The scanning electron photomicrographs of the of the sintered pellets of  $Ba_2Ti_9O_{20}$  at (a) 1000°C for 4 hr. and (b) 1200°C for 2 hr. coated with gold were taken by the JEOL Scanning Electron Microscope, JSM-480A, equipped with a KEVEX ENERGY-DISPERSIVE X-RAY DETECTOR (Fig.4). The particle morphology is found to be almost spherical, with grain size of 0.3– 0.8  $\mu\text{m}$  for the material sintered at 1000°C. However, the grain size is found to increase to 1–3  $\mu\text{m}$  for the sample fired at 1200°C for 2 hrs.

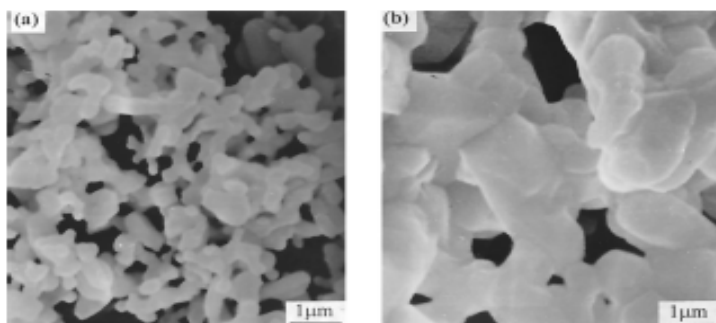


Fig.4: Microstructures of the sintered pellets of  $Ba_2Ti_9O_{20}$  at (a) 1000°C for 4 hr. and (b) 1200°C for 2 hr.

### 3.5 Dielectric Constant Measurement

The functional properties of the dielectric ceramic samples, Polarizability and Dielectric Constant were determined at high-frequency by means of a Hioki measuring apparatus with a parallel plate arrangement. The test samples were taken in cylindrical shape of 6 mm in diameter and 4 mm in height and were fitted in a fixture bounded by metallic walls at its two flat faces. The dielectric constant can be determined accurately from DR dimensions and the resonance frequency as measured on a network analyzer. Table 1 below lists the obtained values of Quality factor (Q) and dielectric Constants at 6 GHz frequency along with the densities of sintered samples determined using the conventional method of Archmede's Principle.

Sintering Temperature/ Time	Density ( $\text{g}/\text{cm}^3$ )	Q (6 GHz)	$\epsilon_r$ (6 GHz)	$\epsilon_r$ (10 GHz)
1000°C for 4 hr.	4.3	3200	36	34.5
1200°C for 2 hr.	4.4	3560	38	39

**Table 1: Properties of Sintered  $Ba_2Ti_9O_{20}$  Dielectric Ceramics**

## 4 Conclusions

The Internal Combustion Method has been successfully employed to synthesize the complex titanates based Dielectric Resonator (DR) materials. The realization of monophasic complex titanates;  $Ba_2Ti_9O_{20}$  had been a challenge since long. In the present work, we have developed Ca doped Di-barium Nonatitanate ( $Ba_{1-x}/Ca_x)_2Ti_9O_{20}$  through formation of nano sized powder of intermediate phases of  $(Ba/Ca)Ti_4O_9$  and  $TiO_2$  with carbonaceous material. This powder when calcined at 600°C and sintered at 1200°C for 2 hrs. after pelletization, produced a dense and phase pure  $(Ba/Ca)_2Ti_9O_{20}$  Barium Nonatitanate. The synthesized materials were found to have dielectric characteristics that qualify them to be used as Dielectric Resonator in Microwave Communication Technology.

### References

- [1] Maria, M. Amala Sekar, Sundar Manoharan, S. and Patil, K.C., 1990, J. Mater. Sci. Lett., 9, p.1205.
- [2] Kingsley, J.J., Suresh, K. and Patil, K.C., , 1990, J. Mater. Sci., 25, p.1305.
- [3] Purohit, R.D., Saha, S. and Tyagi, A.K., 2001, J. Nucl. Mater., 288, p.7.
- [4] Freer, R., 1993, Silic. Ind., 9.
- [5] Richtmyer, R.D., 1939, J. Appl. Phys., Vol. 10, pp. 391-398.
- [6] Cohn, S.B., 1968, IEEE TMTT, pp. 218-227.
- [7] Plourde, J.K., D. F. Line, H. M. O'Bryan and J. Thomson, 1975, J. Am. Ceram. Soc. 58, p. 418.
- [8] O'Bryan, M. and Thomson, J., 1974, J. Am. Ceram. Soc. 57, p. 450.
- [9] Plourde, J.K. and Ren, C.L., 1981, IEEE TMTT, pp. 754-770.
- [10] Bonetti, R.R. and Atia, A.E., 1981, IEEE TMTT, pp. 1333-1337.
- [11] Bonetti, R.R. and Atia, A.E., 1981a, IEEE TMTT, pp. 323-327.
- [12] Guillon, P. and Garault, Y., 1977, TMTT (MTT-25), pp. 916-922.
- [13] Lu, H.C., Burkhart, L.E., and Schrader, G.L., 1991, J. Am. Ceram. Soc. 74, p.968.
- [14] Petrov, Peter and Alford, Neil McNeill, 2006, United States Patent 7119641, Oct. 10, 2006
- [15] Petrov, Peter and Alford, Neil McNeill, 2005, European Patent EP1527497, April 5, 2005.
- [16] Cava, R.J., 2001, J. Mater. Chem., 11, p.54.

- [17] Lee, C.C. and Lin, P., 1998, *Jpn. J. Appl. Phys.* 37, p.878.
- [18] Choy, J.H. and Han, Y.S., 1995, *J. Am. Ceram. Soc.* 78, p.1167.
- [19] Kim, M., Dahmen, O. and Searcy, A.W., 1987, *J. Am. Ceram. Soc.* 70, p.164.
- [20] Kriechbaum, G.M. and Kleinschmit, P., 1989, *Advanced Materials*, 10, p.330.
- [21] Suwa, Y., Komarneni, S. and Roy, R., 1986, *J. Mater. Sci. Lett.*, 5, p.21.
- [22] Gleiter, H., 1989, *Progress in Materials Science Vol.* 33, pp. 223-315.
- [23] Choy, J.H., Han, Y.S., Kim, J.T. and Ho Kim, Y., 1995, *J. Mater. Chem.*, 5, p.57.
- [24] Purohit, R.D., Tyagi, A.K., 2002, *J. Mater. Chem.*, 12, pp.1218–1221.
- [25] Lin, W.Y., Gergardt, R.A. and Speyer, R.F., 1995, *J. Mater. Sci.*, 34, p.3021.
- [26] Lin, W.Y. and Speyer, R.F., 1999, *J. Mater. Res.*, 14, pp.1939-1943.
- [27] Grigor'eva, L.; Petrov, S.; Sinel'shchikova, O.; Drozdova, I.; Gusarov, V., 2007, *Glass Physics and Chemistry*, 33 (1), pp. 72-79(8).
- [28] Wu S.; Wang G.; Zhao Y.; Su H., 2003, *J. European Ceramic Society*, 23 (14), pp. 2565-2568(4).
- [29] Fang T. T.; Shiue J. T.; Liou S. C., 2002, *J. European Ceramic Society*, 22 (1), pp. 79-85.
- [30] Grigor'eva L.F.; Petrov S.A.; Sinel'shchikova O.Y.; Gusarov V.V., 2003, *Glass Physics and Chemistry*, 29 (2), pp. 188-193.
- [31] Wang H.-W.; Chung M.-R., 2003, *Materials Chemistry and Physics*, 77 (3), pp. 853-859.
- [32] Cerchez M.; Boroica L.; Hülsenberg D., 2000, *Phys. and Chem. of Glasses – Euro. J. Glass Sci. and Tech. B*, 41 (5), pp. 233-235.
- [33] Cheng C.M.; Yang C.F.; Lo S.H.; Tseng T.Y., 2000, *J. European Ceramic Society*, 20 (8), pp. 1061-1067.
- [34] Lin W.Y., Gerhardt R.A., Speyer R.F., Hsu J.Y., 1999, *Journal of Materials Science*, 34 (12), pp. 3021-3025.
- [35] Tang, X.; Liu, J.; Kwok, K.; Chan, H., 2005, *Journal of Electroceramics*, 14 (2), pp. 119-122.
- [36] Maher G.H.; Hutchins C.E.; Ross S.D., 1996, *Journal of Materials Processing Technology*, 56 (1), pp. 200-210.
- [37] Yebin Xu, Yanyan He, Liangbin Wang, 1999, *J. Mater. Res.*, 14, pp.1195-1199.
- [38] Min-Hung Weng and Cheng-Liang Huang, 2000, *Jpn. J. Appl. Phys.*, 39, pp.3528-3529.
- [39] Maria, M. Amala Sekar, Sundar Manoharan, S. and Patil, K.C., 1990, *J. Mater. Sci. Lett.*, 9, p.1205.
- [40] Kingsley, J.J., Suresh, K. and Patil, K.C., 1990, *J. Mater. Sci.*, 25, p.1305.
- [41] Purohit, R.D., Saha, S. and Tyagi, A.K., 2001, *J. Nucl. Mater.*, 288, p.7.
- [42] Purohit, R.D., Tyagi, A.K., Methews, M.D. and Saha, S., 2000, *J. Nucl. Mater.*, 280, p.51.
- [43] Oh, I., Hong, S. and Sun, Y., *J. Mater. Sci.*, 32, p.3177, 1997.
- [44] Schafer, J., Sigmund, W., Roy, S. and Aldinger, F., 1997, *J. Mater. Res.*, 12, p.2518.